



EMPIRICAL WAVELET TRANSFORM BASED CLASSIFICATION OF GLAUCOMA FROM RETINAL FUNDUS IMAGES

Shilpa Kaushal, Sunil Datt Sharma , Shruti Jain*¹

Department of Electronics & Communication Engineering,
Jaypee University of Information Technology, Solan, Himachal Pradesh, India

*Corresponding author E-mail: jain.shruti15@gmail.com

ARTICLE INFO

ABSTRACT

Key Words

Retinal Fundus images,
Empirical Wavelet
Transform, Correntropy,
Support Vector Machine,
Intraocular pressure



Glaucoma is termed as the second most common disease which leads to blindness. The main cause of glaucoma is an increase in the pressure of fluid present inside an eye. If not detected at embarkation stage, can lead to complete vision loss. Early stage detection of glaucoma can decrease the risk of blindness and save the vision. In general, there are various texture features but in this paper study of the empirical wavelet transform (EWT) has been done on fundus images for early detection of glaucoma. Quantitative analysis and classification of these features give the cross-validation accuracy of 98.3% using fivefold.

INTRODUCTION

The most frequent causes of blindness are Glaucoma. Glaucoma is the damage of nerve fibers that leads to the formation of small non-seeing areas in field of vision. Permanent blindness results when the entire nerve is destroyed. This damage is a result of intraocular pressure (IOP) or aqueous humor proliferation [1, 2]. Amount of fluid produced inside an eye, produces the amount of fluid that flows out of eye thereby keeping pressure within the safe range. Increase in this pressure damages the optic nerve. Average IOP in adults is 16mmHg while the range can be defined between 9mmHg to 21mmHg. In glaucoma, pressure of the eye increases up to 26mm Hg, which can leads to the blur

in the vision. If the IOP goes above 30mmHg then the result is vision loss [3]. In the detection of Glaucoma at clinical level, different tests like Tonometry (measure of IOP), Pachymetry (measure of central corneal thickness), Gonioscopy (inspect of drainage of eye), Ophthalmoscopy (optic nerve head damage evaluation), Parimetry(test the visual field of eye) etc.[4]. These tests are costly and require trained persons. Various authors have proposed the different methods to identify the Glaucoma disease. Krishnan *et al.* prospective a method to detect the glaucoma and achieved the classification accuracy of 91.67% using Support Vector Machine (SVM) [5].

Nyul *et al.*[6] suggested a method in which the pre-processing stage comprises the normalization, illumination correction, & vessel improvement and generic method has been used for the features extraction. On the extracted features classification accuracy is 80% using SVM. A method proposed by Bock *et al.* for glaucoma detection (GD), which uses the standard pattern recognition pipeline and 86% accuracy achieved with SVM classifier[7]. Mookiah *et al.*[8] determined an automatic detection method for GD and 95% accuracy have been achieved using SVM classifier. This is useful for the Early GD. Dua *et al.*[9] proposed a method in which energy based feature are used to classify the glaucoma and accuracy of this method was 93% with SVM and naive Bayes classifiers with tenfold validation. A method proposed by Beaula *et al.*[10] utilized correntropy features Empirical Wavelet Transform(EWT) with t-test for the glaucoma detection and tenfold cross validation accuracy is 96.6% with the LS-SVM. Patil *et al.*[11] proposed a method in which cup disk ratio (CDR) for feature extraction, and image filtration and color contrast improvement for pre-processing have been used for the GD. Dey *et al.* [12] determined a method for GD in which contrast enhancement and removal of noise are used for pre-processing, Principal Component Analysis (PCA) for feature extraction and SVM for classification. The cross validation accuracy of the method proposed by Dey *et al.* is 96%. Singh *et al.*[13] prospective a method in which the 97% has been achieved. This method uses the pre-processing, feature extraction and SVM classifier for the GD. Rest of the paper is divided as follows: In Section II various steps involved in detection of Glaucoma and Normal image have been presented, summary of different methods discussed in Section III. The paper has concluded in section IV.

MATERIALS AND METHODS

In this study, the decomposition of the fundus glaucoma images has done using EWT and then the correntropies of the decomposed images have calculated and these correntropies were applied for the student *t*-test algorithm subjected to SVM classifier. A detail of the studied algorithm is shown in Figure 1.

2.1 Collection of Data: The images [14] used for the research of an algorithm was collected from the public database, "Medical Image Analysis Group"[15]. In this database, there are total 455 colour fundus images in which 255 are normal and remaining 250 are Glaucoma. Available images are saved in 24-bit JPEG file format at various resolutions. From total 455 images, only 50 glaucoma and 50 normal images is taken for the implementation of the method.

2.2 Pre-Processing Method: Pre-processing is a term defined for procedure with images at the lowest level of operation of any method [16]. The main objective of pre-processing is enhancement of an image data that suppresses unwilling distortions or image features important for processing, while geometric transformation of images are classified among pre-processing methods [17]. In this paper, 2D channel component, i.e. Red, Green, Blue and Gray scale components were extracted from the RGB 3D fundus image.

2.3 Feature Extraction Method : Feature extraction is a process used to transfigure recognizable non- detectable and detectable features into corresponding terminologies[18]. Extraction of basic features like spot, edge, wave and ripple from the normal or gray level images comes under the techniques employed in feature extraction method [19].

EWT has been used as a wavelet technique for the feature extraction because in this wavelet transform, filter bank is constructed from the detected Fourier boundaries obtained from processed signal. In this process, no assumptions are made about the configuration of the signal [20]. The EWT target disintegrated a signal / an image on wavelet tight frames that are built adaptively [21]. EWT is an adaptable because in the analysed signal, filter support depends upon the area where the information is present. Features of empirical wavelet also includes the equivalent dilation factors which do not follow a set of scheme but are detected empirically [22]. In EWT, the Fourier spectrum range 0 to π is divided into P number of parts where divided parts are termed as segment. Limit of each segment is given by ω_p , ranging from $\omega_0 = 0$ and $\omega_p = \pi$. The transition phase T_p depends upon ω_p which has width of $2f_p$, where $f_p = a \omega_p$ for $0 < a < 1$ [23]. Empirical wavelets are defined on each neighbouring section by the constructed filter bank. The empirical wavelets $\zeta_p(X)$ and the empirical scaling function $\xi_p(X)$ is described by Eq. (1) and Eq. (2) [24].

$$\zeta_p(X) = \begin{cases} 1 & \text{if } (1+a)\omega_p \leq |X| \leq (1-a)\omega_{p+1} \\ \cos\left[\frac{\pi}{2}Y(a, \omega_{p+1})\right] & \text{if } (1-a)\omega_{p+1} \leq |X| \leq (1+a)\omega_{p+1} \\ \sin\left[\frac{\pi}{2}Y(a, \omega_p)\right] & \text{if } (1-a)\omega_p \leq |X| \leq (1+a)\omega_p \\ 0 & \text{otherwise} \end{cases} \quad (1)$$

and

$$\xi_p(X) = \begin{cases} 1, & \text{if } |X| \leq (1-a)\omega_p \\ \cos\left[\frac{\pi}{2}Y(a, \omega_p)\right], & \text{if } (1-a)\omega_p \leq |X| \leq (1+a)\omega_p \\ 0, & \text{otherwise} \end{cases} \quad (2)$$

where $Y(a, \omega_p)$ and $Y(a, \omega_{p+1})$ are defined by equation (3) and (4) respectively.

$$Y(a, \omega_p) = F\left(\frac{1}{2a\omega_p} (|X| - (1-a)\omega_p)\right) \quad (3)$$

$$Y(a, \omega_{p+1}) = F\left(\frac{1}{2a\omega_{p+1}} (|X| - (1-a)\omega_{p+1})\right) \quad (4)$$

2D EWT can be classified as: 2D Curvelet EWT, 2D Ridgelet EWT, 2D Tensor EWT, and 2D Littlewood Paley [25]. In this paper, 2D Littlewood Paley EWT is used as the image decomposition method.

i) Algorithm for EWT 2D Little-wood Paley:

INPUT: Extracted channel images $h(x)$.

OUTPUT: Sub-band images $Y_g^{\text{eLWP}}(n, x)$.

START

STEP 1: Calculation of Average Pseudo Polar FFT : Compute average Pseudo-Polar FFT $F_P(\overline{|\omega|})$ using Eq. (5)

$$F_P(\overline{|\omega|}) = \frac{1}{N_\theta} \sum_{i=0}^{N_\theta-1} |F_P(g)(\theta_i, |\omega|)| \quad (5)$$

Where $F_P(g)(\theta_i, |\omega|)$ is the Pseudo-Polar FFT taking average w.r.t. θ_i in which i_{th} Fourier boundary angle $\epsilon [0, \pi]$ and N is the number of filter segments.

STEP 2: Design of Filter bank B : Bank B is build by performing Fourier boundaries detection on average Pseudo-Polar FFT.

$$B = \{\phi_1(x), \{\psi_n(x)\}_{n=1}^{N-1}\} \quad (6)$$

Where $\phi_1(x)$ and $\psi_n(x)$ are filter bank parameters.

STEP 3: Sub band images : Sub band images are obtained by passing extracted channel image $h(x)$ from filter bank B and

$Y_g^{eLWP}(n, x)$ is the sub band images of n^{th} EWT Littlewood Paley component.

END: From the obtained sub-band images, correntropy is calculated which has been used as the feature for the detection of Glaucoma.

ii) **Correntropy:** Correntropy is a kernel-based measure of signals those are non-linearly mapped into a feature space. It preserves both temporal and statistical information present in the signal. This method can also be used to find the texture distribution of the processed image components [26]. Value of kernel in the correntropy reduces to the expected value of kernel of choice. The kernel, which is extensively used, is Gaussian kernel [27]. Gaussian kernel was used in the calculation of the correntropy value because the correntropy estimation is done on the finite number of samples, which sets subsidiary leap on the kernel size. Therefore, by using the Gaussian kernel, probability density function obtained is smooth in the non-linear mapping. $k(x_s, x_t)$ is the Gaussian function expressed by Eq. (7).

$$k(x_s, x_t) = \frac{1}{\sqrt{2\pi}\sigma^2} \exp\left(-\frac{\|x_s - x_t\|^2}{2\sigma^2}\right) \quad (7)$$

σ Is the size of the kernel used. The correntropy value $V(s, t)$ is represented by Eq. (8) :

$$V(s, t) = \sum_{n=0}^{\infty} \frac{(-1)^n}{2^n \sigma^{2n} n!} E \|x_s - x_t\|^{2n} \quad (8)$$

Number of correntropy features lean on the value of Gaussian kernel parameter and in the computation of correntropy, the value of n is taken as 1. [27]

2.4 Feature Selection: For the selection of the features, student t -test algorithm is used. In this algorithm, highest rank value is being selected and then used for the further classification process. Normal Distribution is used for the test [28]. The highest values of correntropy features are normalized using z -score normalization [29].

2.5 Classification: The way toward gathering the testing into the relating classes is known as arrangement of dataset. SVM classifier can characterize both straight and non-direct order. With the assistance of the accessible preparing information, it makes the hyper plane between the classes which brings about great division accomplishment instinctively however the sets that are accessible to separate are not directly distinguishable in the space. In non-direct order module, the information is mapped from input space to higher dimensional element space by utilizing the information, which is mapped into the part work [30]. The Gaussian spiral work is utilized for grouping the information.

RESULTS AND DISCUSSION

For the implementation of the method, the data has been collected from different databases available that are discussed in section 2.1. After the collection of images, they are pre processed. Figure 2 shows the extracted red, green, blue and gray scale channels of the Glaucoma image and Normal eye image.

After the pre-processing step, an image was subjected to the feature extraction where EWT is used as the wavelet transform for the decomposition of an

image. Figure 3 shows the frequency spectrum of the glaucoma and normal image. For different images, the frequency spectrum is also different. Figure 4 and Figure 5 shows the EWT components of gray, red, blue and green channels which are obtained for the Glaucoma and Normal images respectively. After the pre-processing step, an image was subjected to the feature extraction where EWT is used as the wavelet transform for the decomposition of an image. Figure 3 shows the frequency spectrum of the glaucoma and normal image. For different images, the frequency spectrum is also different. Figure 4 and Figure 5 shows the EWT components of gray, red, blue and green channels which are obtained for the Glaucoma and Normal images respectively. After calculating EWT

components, correntropy features were computed. These features are levy to *t*-test as a feature selection process. All the *t*-values were placed in the tabular form and the values are sorted in the descending order. The above six values are selected on which classification process is applied. Table 1 to Table 4 represents the six highest values of correntropy features for gray channel, red channel, green channel, and blue channel respectively. In table 1 to table 4, ce_{xy} is correntropy value of 'y' image and 'x' EWT component. After feature selection step, the SVM classifier is applied where the cross validation accuracy of 98.3% is obtained using fivefold. Table 5 represents various approaches for GD that is correlated with the outcome obtained from aforementioned methods.

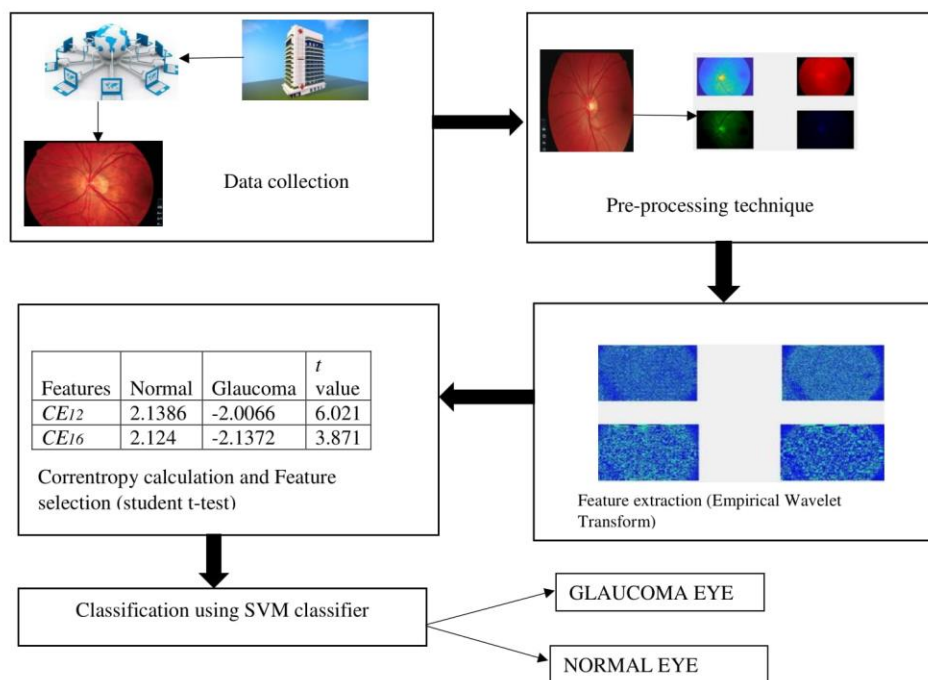


Figure 1: Flow chart of the method discussed in the paper for the detection of Glaucoma

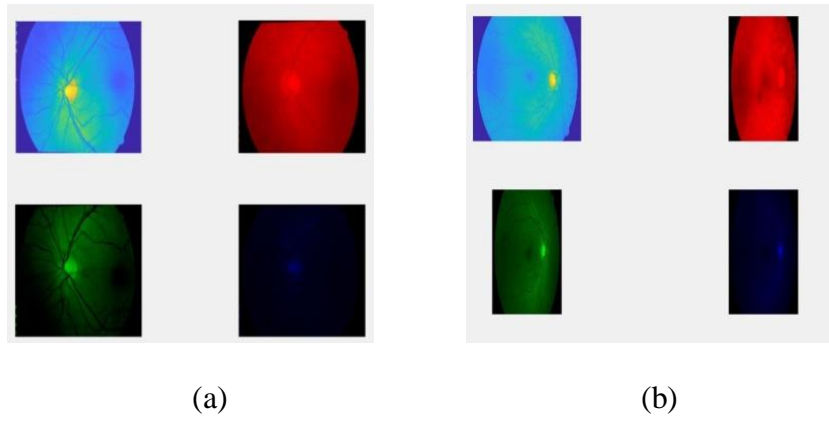


Figure 2: Gray, Red, Green and Blue channel of the (a) Glaucoma eye image (b) Normal eye image

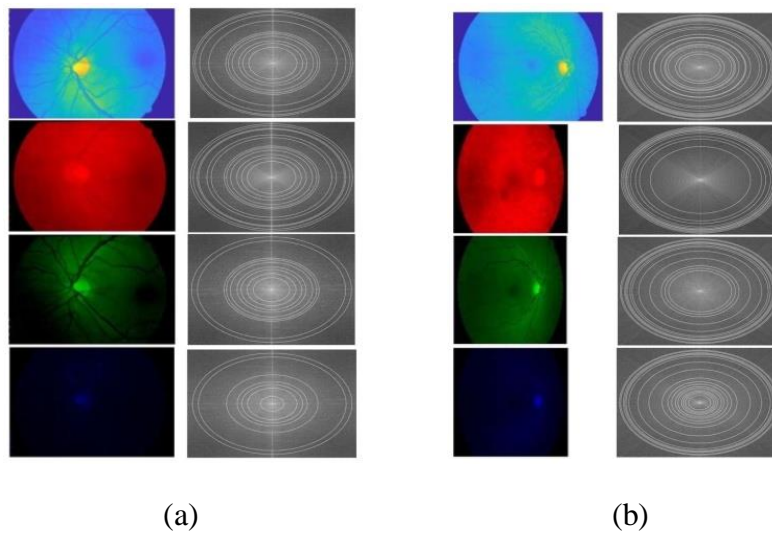


Figure 3: Frequency Spectrum of Gray, Red, Green and Blue channel of the (a) Glaucoma image (b) Normal image

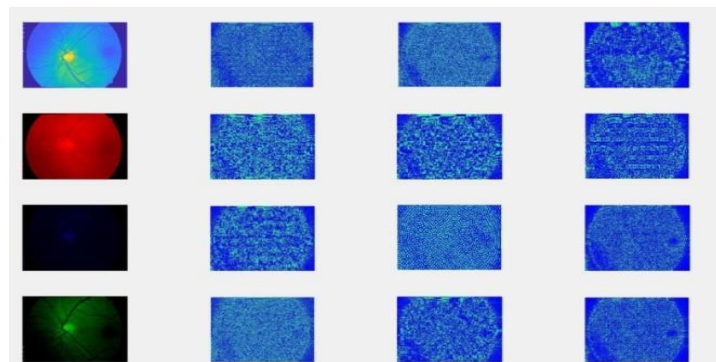


Figure 4: EWT components of the Gray, Red, Blue and Green channel of the Glaucoma image.

Table1: Correntropy values of Gray channel based on highest *t*- value.

Features	Normal	Glaucoma	<i>t</i> value
<i>ce</i> ₃₂	3.95	-0.049	5.73
<i>ce</i> ₅₆	2.95	-1.68	3.46
<i>ce</i> ₁₅	2.14	-1.33	2.14
<i>ce</i> ₃₄	1.72	-1.37	1.75
<i>ce</i> ₄₅	3.46	-4.27	1.56
<i>ce</i> ₂₃	2.35	-2.37	0.99

Table 2: Correntropy values of Red channel based on highest *t*- value.

Features	Normal	Glaucoma	<i>t</i> value
<i>ce</i> ₃₁	2.46	-2.44	4.86
<i>ce</i> ₃₃	1.33	-2.91	4.31
<i>ce</i> ₂₅	2.65	-0.79	3.18
<i>ce</i> ₁₃	1.23	-1.27	2.16
<i>ce</i> ₂₂	2.37	-1.26	2.02
<i>ce</i> ₅₁	3.26	-1.96	1.56

Table 3: Correntropy values of Green channel based on highest *t*- value.

Features	Normal	Glaucoma	<i>t</i> value
<i>ce</i> ₆₂	2.05	-2.047	3.61
<i>ce</i> ₁₅	1.09	-1.087	3.01
<i>ce</i> ₄₆	0.45	-0.47	1.48
<i>ce</i> ₃₂	1.79	-1.69	1.41
<i>ce</i> ₅₄	2.37	-1.23	1.21
<i>ce</i> ₂₁	3.27	-0.23	0.46

Table 4: Correntropy values of Blue channel based on highest *t*- value.

Features	Normal	Glaucoma	<i>t</i> value
<i>ce</i> ₂₅	2.14	-2.01	6.02
<i>ce</i> ₆₂	2.12	-2.14	3.87
<i>ce</i> ₁₂	0.53	-0.55	2.06
<i>ce</i> ₃₆	0.88	0.88	1.03
<i>ce</i> ₅₂	2.32	-2.32	1.00
<i>ce</i> ₄₃	1.24	-1.24	0.95

Table 5: Comparison of different methods proposed for the detection of Glaucoma

Authors	Methods	Images Number	Images Database taken	Features considered	Classification Method	Accuracy (%)
Implemented work	Texture features based	Glaucoma:50 Normal:50	Publically available database http://medimrg.webs.ull.es	Corr-entropy	Support Vector Machine	98.3
Krishnan et al [5]	Texture features , DWT energy and HOS features based	Glaucoma:30 Normal:30	Confidential data base Kasturba Medical College, Manipal, India	Higher order statistics and energy	Support Vector Machine	91.6
Nyul et al [6]	-	NA	-	Principal component analysis	Support Vector Machine	80
Bock et al [7]	Texture features based	NA	-	Fast Fourier transform coefficients, and intensity of pixels.	Support Vector Machine	86
Mookiah et al [8]	NA	NA	-	Higher order statistics and wavelet features	Support Vector Machine	95
Dua et al [9]	Texture feature based	Glaucoma:30 Normal:30	Confidential data base Kasturba Medical College, Manipal, India	Energy features	Support Vector Machine	93.33
Beaula et al[10]	Texture feature based	NA	-	Corr-entropy	Least Square-Support Vector Machine	96.6
Patil et al [11]	Cup Disk Ratio	NA	-	Cup Disk Ratio	Support Vector Machine	NA
Dey et al [12]	NA	NA	-	NA	Support Vector Machine	96
Singh et al [13]	-	Glaucoma:110 Normal:110	Publically available database http://www.tf.fau.de/	Red, Green and Blue values	Support Vector Machine	97

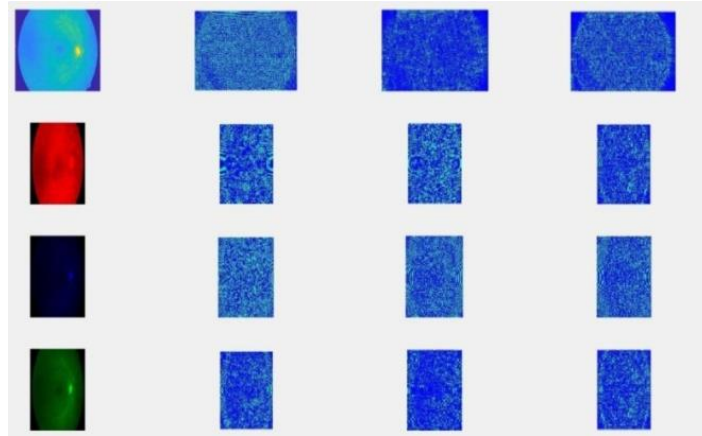


Figure 5: EWT components of the Gray, Red, Blue and Green channel of the Normal image.

CONCLUSION

Glaucoma characterized by neuro degeneration of the optic nerve is one of the common causes of blindness. Restoration of the deteriorated nerve fibers of the optic nerve is difficult thus early detection and succeeding treatment for Glaucoma is necessary to avoid visual loss. Early treatment for glaucoma can decrease the rate of blindness by about 50%. This paper presents a method in which EWT is used as feature extraction technique. Correntropy features are extracted and features with the highest t values are used for the classification process. In this paper we have used SVM classifier. The results obtained from the implemented method are compared with our technique where our method gives the highest accuracy of 98.3% using fivefold cross validation. It can be bringing down to curtain that EWT serves as a potent method for early stage detection of glaucoma. This paper compares different techniques given by different authors. This method can be extended for the detection of other diseases at early stage like Diabetics retinopathy, ovarian cancer and Fatty liver detection.

REFERENCES

1. <https://www.glaucoma.org/research/optic-nerve-regeneration-1.php>
2. Hirschberg, J.-In Graefe-Saemisch, 2te. Aufl. Bd. 14, Abth. 1, S. 122, Leipzig, 1911.
3. GBD 2015 Disease and Injury Incidence and Prevalence, Collaborators. (8 October 2016). "Global, regional, and national incidence, prevalence, and years lived with disability for 310 diseases and injuries, 1990–2015: a systematic analysis for the Global Burden of Disease Study 2015". *Lancet*. 388 (10053): 1545–1602
4. <https://www.glaucoma.org/glaucoma/normal-tension-glaucoma.php>
5. Krishnan, M. R., & Faust, O. (2013). Automated glaucoma detection using hybrid feature extraction in retinal fundus images. *Journal of Mechanics in Medicine and Biology*, 13(01), 1350011
6. Nyúl, (2009, October). Retinal image analysis for automated glaucoma risk evaluation. In *Proc. of SPIE Vol (Vol. 7497, pp. 74971C-1)*.
7. Bock, J. Meier, L. G. Nyl, and G. Michelson, "Glaucoma risk index: Automated glaucoma detection from color fundus images," *Med. Image Anal.*, vol. 14, pp. 471–481, 2010

8. Mookiah, U. R. Acharya, C. M. Lim, A. Petznick, and J. S. Suri, "Data mining technique for automated diagnosis of glaucoma using higher order spectra and wavelet energy features," *Knowl.-Based Syst.*, vol. 33, pp. 73–82, 2012.
9. Dua, Acharya., Chowriappa, & Sree, S. V. (2012). Wavelet-based energy features for glaucomatous image classification. *Ieee transactions on information technology in biomedicine*, 16(1), 80-87.
10. Beaula., M Asirvatham., T Kalimuthu. , "Earlier Detection of Glaucoma using Empirical Wavelet Transform" , *International Journal for Research in Applied Science & Engineering Technology (IJRASET)* , vol 5 , pp 1311-1316 , Apr 2017.
11. Patil, V.S Kamkhedhar. , "Analysis of Human Retinal Images for Automated Glaucoma Screening" , *International Journal for Research in Applied Science & Engineering Technology (IJRASET)* , vol 2 , pp 371-377 , Dec 2014.
12. Dey and S K. Bandyopadhyay, "Automated Glaucoma Detection Using Support Vector Machine Classification Method," 2016, *British Journal of Medicine & Medical Research (BJMMR)*, Kolkata
13. Singh and B. Marakarkandy, (2017). Comparative Study of Glucoma Detection using Different Classifiers.
14. <http://www.ia.uned.es/~ejcarmona/DRIONS-DB.html>
15. <http://medimrg.webs.ull.es/>
16. Pachori, R. Sharma, and S. Patidar, "Classification of normal and epileptic seizure EEG signals based on empirical mode decomposition," in *Complex System Modelling and Control Through Intelligent Soft Computations (ser. Studies in Fuzziness and Soft Computing)*, vol. 319, Q. Zhu and A. T. Azar, Eds. New York, NY, USA: Springer, 2015, pp. 367–388.
17. Pachori and S. Patidar, "Epileptic seizure classification in EEG signals using second-order difference plot of intrinsic mode functions," *Comput. Methods Programs Biomed.*, vol. 113, no. 2, pp. 494–502, 2014.
18. Bhusri, S. Jain and J. Virmani, 2016. Classification of breast lesions using the difference of statistical features, *Research Journal of Pharmaceutical Biological and Chemical Sciences*, 7(4), pp.1365-1372.
19. Rana, S Jain and J Virmani: Classification of Focal Kidney lesions using WaveletBased Texture Descriptors. *International J of Pharma and Bio Sciences*. July-Sep 2016. pp. 646-652.
20. Sharma, S Jain, S Bhusri, "Two Class Classification of Breast Lesions using Statistical and Transform Domain features" *Journal of Global Pharma Technology*, 9 (7), 18-24,2017
21. Maharaja and S. Maflin Shaby. "Empirical Wavelet Transform And GLCM Features Based Glaucoma Classification From Fundus Image."
22. Jambholkar, D Gurve. And P.B., Sharma 2015, Application of Empirical Wavelet Transform (EWT) on images to explore Brain Tumor. In *Signal Processing, Computing and Control (ISPPCC)*,

- September. 2015 International Conference, pp. 200-204.
23. <https://jegilles.sdsu.edu/ewt.html>
24. Maheshwari, Pachori, and U.R. Acharya, 2017. Automated diagnosis of glaucoma using empirical wavelet transform and correntropy features extracted from fundus images. *IEEE journal of biomedical and health informatics*, 21(3), pp.803-813.
25. Gilles, 2013. Empirical wavelet transform. *IEEE transactions on signal processing*, 61(16), pp.3999-4010.
26. Gilles, G. Tran, and S. Osher, 2014. 2D empirical transforms. Wavelets, ridgelets, and curvelets revisited. *SIAM Journal on Imaging Sciences*, 7(1), pp.157-186.
27. Gunduz and J.C. Principe, 2009. Correntropy as a novel measure for nonlinearity tests. *Signal Processing*, 89(1), pp.14-23.
28. Santamaría, P.P. Pokharel, and J.C. Principe, 2006. Generalized correlation function: definition, properties, and application to blind equalization. *IEEE Transactions on Signal Processing*, 54(6), pp.2187-2197.
29. Acharya, Vidya, D.N. Ghista, W.J.E. Lim, F. Molinari, and M. Sankaranarayanan, 2015. Computer-aided diagnosis of diabetic subjects by heart rate variability signals using discrete wavelet transforms method. *Knowledge-based systems*, 81, pp.56-64.
30. Dunham, 2006. Data mining: Introductory and advanced topics. Pearson Education India.
31. Virmani V Kumar, N Kalra and N Khandelwal: SVM based characterization of liver cirrhosis by singular value decomposition of GLCM matrix. *International J of Artificial Intelligence and Soft Computing*. 2013. vol. 3. pp. 276-296.
32. Jain, 2018. Classification of Protein Kinase B using discrete wavelet transforms. *International Journal of Information Technology*, 10(2), pp.211-216.
33. Jain, S.V Bhooshan, and P.K. Naik, 2011. Mathematical modelling deciphering balance between cell survival and cell death using Insulin. *Network Biology*, 1(1), p.46.